

# On population extinction risk in the aftermath of a catastrophic event

Michael Assaf<sup>1</sup>, Alex Kamenev<sup>2</sup>, Baruch Meerson<sup>1</sup>

<sup>1</sup> *Racah Institute of Physics, Hebrew University of Jerusalem, Jerusalem 91904, Israel*

<sup>2</sup> *Department of Physics, University of Minnesota, Minneapolis, Minnesota 55455, USA*

We investigate how a catastrophic event increases the extinction probability of an isolated self-regulated population whose dynamics is governed by a stochastic birth-death process. Using the simple Verhulst logistic model as an example, we combine the probability generating function technique with an eikonal approximation to evaluate the exponentially large increase in the extinction probability caused by the catastrophe. This quantity is given by the eikonal action computed over “the optimal path” (instanton) of an effective classical Hamiltonian system with a time-dependent Hamiltonian. For a general catastrophe the eikonal equations can be solved numerically. For simple models of catastrophic events analytic solutions can be obtained. One such solution becomes quite simple close to the bifurcation point of the Verhulst model. The eikonal results for the increase in the extinction probability caused by a catastrophe agree well with numerical solutions of the master equation.

PACS numbers: 05.40.-a, 87.23.Cc, 02.50.Ga

## I. INTRODUCTION

Evaluation of the extinction risk of a population in the aftermath of a catastrophe - a drastic deterioration of environmental conditions - is of great importance in population biology [1]. A practical approach to modeling of this problem assumes that the population dynamics is governed by a (Markov) stochastic birth-death process [2, 3], and the catastrophe introduces an explicit (and possibly strong) time dependence into one or more of the transition rates. The question we want to address in this work is the following: What is the extinction probability of the population at the time the catastrophic event is over and the environmental conditions return to normal? The explicit time dependence of the transition rates, brought about by the catastrophe, makes the problem difficult for analysis. We will present here a formalism that helps develop an insight into this class of problems. As a prototypical example of the population dynamics we will adopt a simple stochastic Verhulst logistic model. We will be interested in the regime of parameters where, if there is no catastrophe, a long-lived quasi-stationary distribution of the population sizes is formed. Because of the presence of an absorbing state at zero the population ultimately goes extinct in this model even without a catastrophe. A natural measure of the extinction is  $\mathcal{P}_0(t)$ : the probability that the population goes extinct by the time  $t$ . The focus of attention in this work is on the *increase* in the extinction probability  $\mathcal{P}_0(t)$  caused by the catastrophe, see Fig. 1. We will assume that, if there is no catastrophe, the mean time to extinction (MTE) is too long to be relevant. Let  $\mathcal{P}_0^B(t)$  be the extinction probability before the catastrophe occurred. Neglecting a transient related to the relaxation to the quasi-stationary distribution (and the exponentially small extinction probability during this stage), this probability grows very slowly according to  $\mathcal{P}_0^B(t) \simeq 1 - e^{-t/\tau}$ , see *e.g.* [4, 5, 6]. Here  $\tau$  is the MTE if there is no catastrophe. During the catastrophe, which starts at  $t = t_c$ , the extinction probability

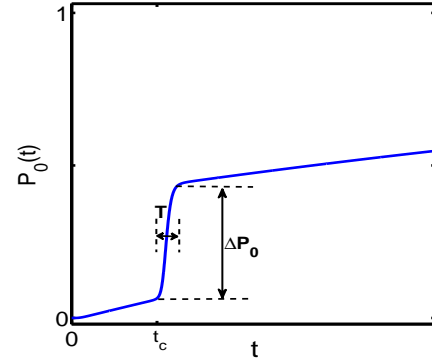


FIG. 1: (Color online.) A schematic plot of the time-dependent extinction probability  $\mathcal{P}_0(t)$  showing the effect of a catastrophe with a characteristic duration  $T$ .

ity  $\mathcal{P}_0(t)$  grows more rapidly and, after the catastrophe, reaches a value  $\mathcal{P}_0^*$ . From then on (again, neglecting a relaxation transient), the extinction probability grows very slowly, approximately as  $\mathcal{P}_0^A(t) \simeq 1 - (1 - \mathcal{P}_0^*)e^{(t_c - t)/\tau}$ . We assume that the effect of the catastrophe is not too weak,  $\mathcal{P}_0^* \gg \mathcal{P}_0^B$ , where  $\mathcal{P}_0^B$  is the (exponentially small) accumulated extinction probability before the catastrophe. The goal of this work is to evaluate the increase of the extinction probability  $\Delta\mathcal{P}_0 \equiv \mathcal{P}_0^* - \mathcal{P}_0^B$ .

The formalism that we will employ to achieve this goal begins from a transformation of the master equation (with time-dependent transition rates) into an exact evolution equation for the probability generating function. For the problem in question this equation is a second-order linear partial differential equation (PDE). We then apply a time-dependent eikonal approximation to this evolution equation. This approximation, in many ways similar to the time-dependent WKB approximation in quantum theory [7], brings the second-order PDE to a first-order PDE of Hamilton-Jacobi type, with an ef-

fective classical Hamiltonian which explicitly depends on time. The further analysis deals with the characteristic lines of the Hamilton-Jacobi equations: the phase trajectories generated by the effective classical Hamiltonian. We will assume throughout the paper that both the initial population size, and the expected population size immediately after the catastrophic event, are much larger than unity. Under this assumption (and not too close to the bifurcation point of the Verhulst model, see below) we will evaluate the (exponentially large) net increase  $\Delta\mathcal{P}_0$  in the extinction probability caused by the catastrophe. This formalism yields an asymptotically correct value of the corresponding large exponent which makes it advantageous compared to the widely used van Kampen's system size expansion of the master equation and related methods, see *e.g.* [2, 3]. Indeed, as it is well established by now, the Fokker-Planck equation, resulting from the van Kampen's system size expansion, cannot predict the MTE of stochastic birth-death systems with exponential accuracy. This can be traced to the failure of the Fokker-Planck equation in describing the actual probability distribution tails of these systems [4, 5, 6, 8, 9].

Here is the layout of the remainder of the paper. We begin Sec. II with a brief reminder on the stochastic Verhulst logistic model. Then we derive the evolution equation for the probability generating function and employ an eikonal approximation in order to determine the MTE of the population if there is no catastrophe. Here our results coincide, with exponential accuracy, with those of previous works on the stochastic Verhulst logistic model. Section III deals with the effect of a catastrophic event on the population survival. We first demonstrate the efficiency of the eikonal method by finding numerically the most probable path to extinction, and computing the corresponding increase in the extinction probability due to the catastrophe, for a typical example of a catastrophic event. Then we obtain non-perturbative (in the catastrophe magnitude) analytical results by adopting a simple schematic form of the catastrophic event: we postulate that the reproduction rate of the population drops instantaneously to zero at a specified time and recovers to the pre-catastrophe value, again instantaneously, after a given time  $T$  has elapsed. Section IV compares our numerical and analytical eikonal results for the extinction probability with direct numerical solutions of the master equation. A brief summary and discussion of our results is presented in Sec. V.

## II. VERHULST MODEL, PROBABILITY GENERATING FUNCTION AND EIKONAL APPROXIMATION

As a prototypical example of self-regulating dynamics of an isolated population we consider the stochastic version of the Verhulst logistic model: a Markov single-step birth-death process. If there is no catastrophe, the

reproduction and death rates are given by

$$\lambda_n = Bn \quad \text{and} \quad \mu_n = n + \frac{Bn^2}{N}, \quad (1)$$

respectively, where we use the same notations as in Ref. [9]. The reproduction rate per individual is constant, while the death rate per individual is constant at small population sizes, but grows proportionally to the population size when the latter is sufficiently large, accounting, for example, for competition for resources. For brevity, time and the transition rates in Eq. (1) are rescaled with respect to the value of the death rate at small population sizes.

At the level of deterministic modeling, the dynamics of the population size is described by the rate equation

$$\dot{n}(t) = (B - 1)n(t) - \frac{B}{N}n^2(t). \quad (2)$$

For  $B > 1$  this equation has an attracting fixed point  $n_s = N(1 - 1/B)$  and a repelling fixed point  $n_0 = 0$ . Throughout the paper we assume  $n_s \gg 1$ ; this necessarily requires  $N \gg 1$ . A linear stability analysis of Eq. (2) around  $n = n_s$  yields the characteristic relaxation time  $\tau_0 = (B - 1)^{-1}$  (in the units of the death rate at small population sizes).

Demographic stochasticity in the Verhulst model is accounted for by the master equation

$$\begin{aligned} \frac{d\mathcal{P}_n}{dt} = & B(n-1)\mathcal{P}_{n-1} - Bn\mathcal{P}_n \\ & + \left[ n + 1 + \frac{B(n+1)^2}{N} \right] \mathcal{P}_{n+1} - \left( n + \frac{Bn^2}{N} \right) \mathcal{P}_n, \end{aligned} \quad (3)$$

where  $\mathcal{P}_n(t)$  is the probability that the number of individuals at time  $t$  is  $n$ . The stochastic Verhulst model, as described by Eq. (3), and related models were considered in many works, see [9, 10, 11, 12, 13, 14] and references therein. It was found that, under certain conditions specified below, a long-lived quasi-stationary distribution, conditioned on non-extinction, is formed in this system after the relaxation time  $\mathcal{O}(\tau_0)$ . The quasi-stationary distribution has a peak with relative width proportional to  $N^{-1/2}$  around the attracting state  $n_s$  of the deterministic description. At much longer times, however, the population goes extinct. This is because  $n = 0$  is an absorbing state, so a rare sequence of events brings the process there with certainty. We will work in such a parameter regime that, if there is no catastrophe, the MTE is too long to be relevant. That is, we will be interested in times which, although much longer than the relaxation time  $\tau_0$ , are still much shorter than the MTE of the system without a catastrophe, that is the one described by Eq. (3).

Notice that the same master equation (3) also describes the stochastic dynamics of three chemical reactions:  $A \xrightarrow{\lambda} 2A$ ,  $A \xrightarrow{\mu} \emptyset$ , and  $2A \xrightarrow{\sigma} A$  [15], with rates  $\lambda \equiv B$ ,  $\mu \equiv 1 + B/N$ , and  $\sigma = 2(\mu - 1)$ , respectively. To be specific,

we will use the notation of the Verhulst model in the following.

We will first demonstrate the method on the case when there is no catastrophe. Introduce the probability generating function [2, 3]

$$G(\varphi, t) = \sum_{n=0}^{\infty} \varphi^n \mathcal{P}_n(t), \quad (4)$$

where  $\varphi$  is an auxiliary variable.  $G(\varphi, t)$  encodes all the probabilities  $\mathcal{P}_n(t)$ , as those are given by the coefficients of its Taylor expansion around  $\varphi = 0$ . The generating function obeys the normalization condition

$$G(1, t) = 1 \quad (5)$$

which follows from the conservation of the total probability. The distribution moments can be expressed through the  $\varphi$ -derivatives of the generating function at  $\varphi = 1$ , *e.g.*  $\langle n \rangle(t) \equiv \sum_n n \mathcal{P}_n(t) = \partial_\varphi G(\varphi, t)|_{\varphi=1}$ .

By multiplying Eq. (3) by  $\varphi^n$  and summing over all  $n$  one obtains, after some algebra, an evolution equation for  $G(\varphi, t)$ :

$$\frac{\partial G}{\partial t} = \frac{B}{N} (1 - \varphi) \varphi \frac{\partial^2 G}{\partial \varphi^2} + (\varphi - 1) \left( B\varphi - 1 - \frac{B}{N} \right) \frac{\partial G}{\partial \varphi}. \quad (6)$$

The signature of the (empty) absorbing state is the absence of a term proportional to  $G(\varphi, t)$  in Eq. (6). This immediately brings about the stationary solution  $G(\varphi, t) = 1$  corresponding to the empty state.

In contrast to the Fokker-Planck equation, which is derivable from the master equation (3) by the van Kampen's system size expansion, the starting point of our theory - the evolution equation (6) - is exact. Throughout the rest of the paper we assume  $N \gg B$ . As our main results below are obtained with exponential accuracy, this strong inequality enables us to neglect the term  $(B/N)\partial G/\partial \varphi$ , and Eq. (6) becomes

$$\frac{\partial G}{\partial t} = \frac{B}{N} (1 - \varphi) \varphi \frac{\partial^2 G}{\partial \varphi^2} + (\varphi - 1) (B\varphi - 1) \frac{\partial G}{\partial \varphi}. \quad (7)$$

This second-order PDE can be interpreted as an imaginary-time Schrödinger equation  $\partial G/\partial t = \hat{\mathcal{H}}G$ , where

$$\hat{\mathcal{H}} = \frac{B}{N} (1 - \varphi) \varphi \frac{\partial^2}{\partial \varphi^2} + (\varphi - 1) (B\varphi - 1) \frac{\partial}{\partial \varphi}$$

is the Hamiltonian operator.

In the framework of the spectral theory [5, 6, 16], the solution of the initial value problem for Eq. (7) can be obtained via an expansion in the eigenfunctions of a Sturm-Liouville problem related to the non-Hermitian operator  $\hat{\mathcal{H}}$ . The boundary conditions, needed for this Sturm-Liouville problem, come from the demand of boundedness of the eigenfunctions at the singular points of  $\hat{\mathcal{H}}$ . In this way one obtains a zero eigenvalue  $E_0 = 0$  which describes the true (absorbing) steady state of the system:

extinction of the population. In addition, one obtains a discrete set of negative eigenvalues  $\{E_n\}_{n=1}^{\infty}$  that describe the decay with time of the discrete set of eigenfunctions. The relative weight of each eigenfunction in the expansion is determined, via  $G(\varphi, t = 0)$ , by the initial probability distribution  $\mathcal{P}_n(t = 0)$ . For  $N \gg 1$  (and not too close to the bifurcation point  $B = 1$ ) the higher eigenvalues  $E_2, E_3, \dots$  scale as  $\tau_0^{-1}$ , whereas the fundamental eigenvalue  $E_1$  is exponentially small. Therefore, there are two widely separated time scales in the problem. During the fast relaxation time  $\mathcal{O}(\tau_0)$  the higher modes decay exponentially, and the probability distribution approaches the quasi-stationary distribution (QSD) mentioned above, which is derivable from the fundamental eigenfunction. The exponentially small decay rate of the fundamental mode (and, correspondingly, of the time-dependent metastable distribution that is proportional to the QSD) is equal to the inverse MTE of the system. We checked that, as in other similar systems [5, 6, 16], the spectral theory yields accurate results both for the complete probability distribution and for the MTE, including the pre-exponent, in the catastrophe-free regime. However, the spectral theory cannot accommodate time-dependent transition rates: the main subject of this work. Therefore, in what follows we will use instead the time-dependent eikonal approximation [4]. Although it only gives exponential accuracy, the eikonal approximation is readily generalizable to multi-species problems [17] and, as we will demonstrate shortly, to time-dependent Hamiltonians.

Now we use the eikonal ansatz  $G(\varphi, t) = \exp[-\mathcal{S}(\varphi, t)]$  in the evolution equation (7). As can be checked *a posteriori*,  $\mathcal{S}$  can be written as  $\mathcal{S} = Ns(p, t)$ , where  $s(p, t) = \mathcal{O}(1)$ . Therefore, the term  $(B/N)(1 - \varphi)\varphi \partial_{pp}^2 \mathcal{S} = \mathcal{O}(1)$  is small compared to the other terms which scale as  $N$ . Neglecting it, we arrive at a first-order PDE for  $\mathcal{S}(\varphi, t)$

$$\frac{\partial \mathcal{S}}{\partial t} + \frac{B}{N} (1 - \varphi) \varphi \left( \frac{\partial \mathcal{S}}{\partial \varphi} \right)^2 - (\varphi - 1) (B\varphi - 1) \frac{\partial \mathcal{S}}{\partial \varphi} = 0, \quad (8)$$

that can be interpreted as a Hamilton-Jacobi equation in the momentum representation, where  $\varphi$  is the momentum. Introducing the canonically conjugate coordinate  $q = -\partial \mathcal{S}/\partial \varphi$ , we obtain a one-dimensional classical Hamiltonian flow with the time-independent Hamiltonian

$$\mathcal{H}(\varphi, q) = (1 - \varphi) \left( \frac{B}{N} \varphi q - B\varphi + 1 \right) q. \quad (9)$$

The fact that  $\mathcal{H}(1, q) = 0$  reflects the probability conservation, see Eq. (5), whereas the fact that  $\mathcal{H}(0, \varphi) = 0$  manifests the presence of the absorbing empty state.

It is convenient to shift the momentum  $p = \varphi - 1$ , leaving the coordinate  $q$  unchanged. The new Hamiltonian is

$$H(p, q) = p \left[ -\frac{B}{N} (p + 1) q + B(p + 1) - 1 \right] q, \quad (10)$$

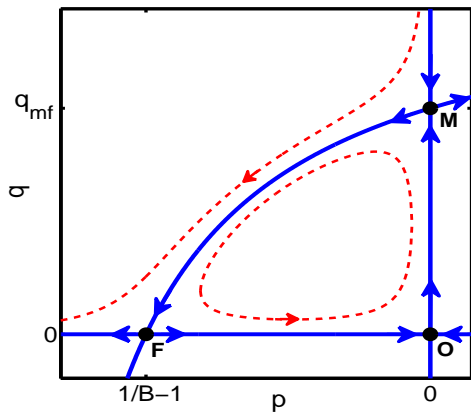


FIG. 2: (Color online.) The phase plane  $(p, q)$  emerging in the eikonal approximation to the stochastic Verhulst model. The fixed points are denoted by  $M$  (the mean-field point),  $F$  (the fluctuational point) and  $0$  (the trivial point). Solid lines depict zero-energy trajectories, including the heteroclinic trajectory  $MF$ . Dashed lines show two examples of non-zero-energy trajectories.

while the Hamilton equations are

$$\dot{q} = \frac{\partial H}{\partial p} = (2p + 1) \left( Bq - \frac{B}{N} q^2 \right) - q, \quad (11)$$

$$\dot{p} = -\frac{\partial H}{\partial q} = -(p^2 + p) \left( B - \frac{2B}{N} q \right) + p. \quad (12)$$

This Hamiltonian flow was investigated, in the context of the three above-mentioned chemical reactions, by Elgart and Kamenev [15]. The phase plane  $(p, q)$ , defined by the Hamiltonian (10), provides a useful visualization of the extinction dynamics, see Fig. 2. As the Hamiltonian does not depend explicitly on time, it is an integral of motion:  $H(p, q) = E = \text{const}$ , and the problem is integrable. The *zero energy* trajectories,  $E = 0$ , play a special role here, as will become clear shortly. One type of zero-energy trajectories are the mean field trajectories, staying on the line  $p = 0$ . Here Eq. (11) becomes

$$\dot{q} = (B - 1)q - \frac{B}{N}q^2 \quad (13)$$

which coincides with the rate equation (2). This fact provides the interpretation of the  $q$ -variable as the reaction coordinate. Importantly, the attracting fixed point of the mean-field, or deterministic line  $p = 0$ ,  $q_{mf} \equiv n_s = N(1 - 1/B)$  becomes a hyperbolic point  $(0, q_{mf})$  of the phase plane  $(p, q)$ . We call this fixed point the mean-field point and denote it by  $M$ .

The Hamiltonian (10) has two more zero-energy lines. One of them is the extinction line  $q = 0$  which includes two more hyperbolic fixed points of the phase plane  $(p, q)$ : the “fluctuational point”  $(1/B - 1, 0)$ , denoted by  $F$ , and the trivial point  $(0, 0)$  denoted by  $0$ . The third zero-

energy curve

$$q = q_0(p) = N - \frac{N}{B(p + 1)}, \quad (14)$$

includes a heteroclinic trajectory that exits, at time  $t = -\infty$ , the mean field point  $M$  along its unstable eigendirection, and enters, at time  $t = \infty$ , the fluctuational point  $F$  along its stable eigendirection. This heteroclinic trajectory represents the optimal (most probable) path, or the instanton connection, of the extinction dynamics. Indeed, it describes, in the eikonal language, the most probable sequence of discrete events bringing the system from its quasi-stationary state to extinction, *cf.* [4, 18, 19, 20]. If there is no catastrophe, the MTE of the population is, with exponential accuracy,  $\tau \sim \exp(\mathcal{S}_0)$ , where the (zero-energy) action is

$$\mathcal{S}_0 = - \int_{-\infty}^{\infty} q \dot{p} dt, \quad (15)$$

and the integration should be performed along the zero-energy heteroclinic trajectory (14). The result is

$$\tau \sim \exp \left[ - \int_0^{\frac{1}{B}-1} q_0(p) dp \right] = \exp \left( N \frac{B - 1 - \ln B}{B} \right). \quad (16)$$

The approximation is valid when  $\mathcal{S}_0 \gg 1$ . One can check that the result (16) coincides, up to a pre-exponent, with those of [9, 11, 14, 21].

Of a special interest is the region of parameters close to the bifurcation point of the Verhulst model:  $N^{-1/2} \ll B - 1 \ll 1$ , where the left inequality is required for the validity of the eikonal approximation. For  $B - 1 \ll 1$  the action

$$\mathcal{S}_0 \simeq \frac{N(B - 1)^2}{2}, \quad (17)$$

scales as the square of the distance to the bifurcation point. It has been found recently [17, 22] that, close to the bifurcation point, the Verhulst model, the SIS (Susceptible - Infected - Susceptible) model of epidemiology [9, 10, 11, 12, 13, 14], the SIS model with demography [22, 23], the SIR (Susceptible - Infected - Recovered) model with demography [17, 24, 25] and other related stochastic models become, in the leading order, *identical* if their rates are properly rescaled. One can check that, in this limit, the term  $-(B/N)pq$  in the square brackets in Eq. (10) can be neglected compared to the rest of the terms, and one arrives at the “universal” Hamiltonian

$$H(p, q) = p \left( -\frac{q}{N} + p + B - 1 \right) q, \quad (18)$$

introduced in Ref. [15] in the context of the three chemical reactions mentioned above. All three zero-energy lines in the phase plane of the universal Hamiltonian are straight lines, and the action  $\mathcal{S}_0$ , given by Eq. (17), is simply the area of the triangle formed by these straight lines.

### III. CATASTROPHIC EVENT AND ACTION CALCULATION

To model a catastrophic event we assume that, because of unfavorable environmental changes, the reproduction rate drops and then recovers to the pre-catastrophe value. This can be described by introducing a time-dependent factor  $f(t)$ , such that  $f(\pm\infty) = 1$ , into the reproduction rate:

$$\lambda_n(t) = Bf(t)n, \quad (19)$$

The death rate  $\mu_n$  remains constant in time in this model, see Eq. (1). At the level of deterministic modeling, the population size is described by the rate equation

$$\dot{n}(t) = [Bf(t) - 1]n(t) - \frac{B}{N}n^2(t), \quad (20)$$

the master equation becomes

$$\begin{aligned} \frac{d\mathcal{P}_n}{dt} &= Bf(t)(n-1)\mathcal{P}_{n-1} - Bf(t)n\mathcal{P}_n \\ &+ \left[ n+1 + \frac{B(n+1)^2}{N} \right] \mathcal{P}_{n+1} - \left( n + \frac{Bn^2}{N} \right) \mathcal{P}_n, \end{aligned} \quad (21)$$

while the evolution equation for  $G(\varphi, t)$  is again an imaginary-time Schrödinger equation  $\partial G/\partial t = \hat{\mathcal{H}}G$  with the Hamiltonian operator

$$\hat{\mathcal{H}} = \frac{B}{N}(1-\varphi)\varphi \frac{\partial^2}{\partial \varphi^2} + (\varphi-1)[Bf(t)\varphi-1] \frac{\partial}{\partial \varphi}$$

that now explicitly depends on time. The same eikonal ansatz  $G(\varphi, t) = \exp[-\mathcal{S}(\varphi, t)]$  brings about the Hamilton-Jacobi equation for  $\mathcal{S}(\varphi, t)$  which defines a classical Hamiltonian flow with the time-dependent Hamiltonian

$$H(p, q, t) = p \left[ -\frac{B}{N}(p+1)q + Bf(t)(p+1) - 1 \right] q, \quad (22)$$

with the same coordinate  $q$  and shifted momentum  $p = \varphi - 1$  as in the time-independent case. The Hamilton equations are

$$\dot{q} = \frac{\partial H}{\partial p} = (2p+1) \left[ Bf(t)q - \frac{B}{N}q^2 \right] - q, \quad (23)$$

$$\dot{p} = -\frac{\partial H}{\partial q} = -(p^2 + p) \left[ Bf(t) - \frac{2B}{N}q \right] + p. \quad (24)$$

As the Hamiltonian  $H$  is not an integral of motion anymore, the problem is in general non-integrable. There are, however, two planes in the extended phase space  $(p, q, t)$  where the Hamiltonian is still conserved and equal to zero. These are the mean-field plane  $(p=0, q, t)$  and the extinction plane  $(p, q=0, t)$ . In the mean-field plane Eq. (11) becomes

$$\dot{q} = [Bf(t) - 1]q - \frac{B}{N}q^2 \quad (25)$$

which again coincides with the rate equation (20). In the eikonal approximation the extinction occurs along the instanton connection of the time-dependent Hamiltonian (22) in the extended phase space  $(p, q, t)$ . To reasonably describe a catastrophe the function  $f(t)$  should be bounded from above. In this case there exists a heteroclinic trajectory  $[p_{op}(t), q_{op}(t)]$  which exits the mean-field fixed point  $M$  well before the catastrophe and arrives at the fluctuational fixed point  $F$  after the catastrophe is over. The full action along this heteroclinic trajectory

$$\mathcal{S} = \int_{-\infty}^{\infty} \{-q_{op}(t)\dot{p}_{op}(t) - H[q_{op}(t), p_{op}(t), t]\} dt \quad (26)$$

[where  $H$  is given by Eq. (22)], determines (the logarithm of) the increase in the extinction probability caused by the catastrophe.

#### A. Instanton calculations: numerical solution

For a smooth  $f(t)$ , the Hamilton equations (23) and (24) (and similar Hamilton equations for other models) can be accurately solved by a shooting method with a single shooting parameter. As in the unperturbed case, the instanton connection must exit, at  $t = -\infty$ , the mean-field point  $M$  and enter, at  $t = \infty$ , the fluctuational point  $F$ . In a numerical solution we specify, at some initial moment of time  $t = t_{in}$  prior to the catastrophe, the coordinate  $q(t_{in})$  and momentum  $p(t_{in}) < 0$  which lie on the *unperturbed* heteroclinic trajectory (14) in a vicinity of the mean-field point  $M$ . The initial momentum  $p(t_{in})$  can play the role of the shooting parameter. It must be chosen sufficiently close to zero for the numerically found instanton to approximate well the entire perturbed instanton. On the other hand, the instanton must reach, at a final time  $t_f$  after the catastrophe, (a close vicinity of) the fluctuational point  $F$ . Therefore, for too a small  $p(t_{in})$ , intrinsic logarithmic slowdown near the fixed point  $t_f$  increases the computation time and causes accumulation of numerical errors. Denoting the numerically found instanton (or optimal path) by  $[p_{op}^{(n)}(t), q_{op}^{(n)}(t)]$ , we can write the action along it as

$$\mathcal{S}_{num} = \int_{t_{in}}^{t_f} \left\{ -q_{op}^{(n)}(t)\dot{p}_{op}^{(n)}(t) - H[q_{op}^{(n)}(t), p_{op}^{(n)}(t), t] \right\} dt. \quad (27)$$

As an example, let us consider

$$f(t) = 1 - \frac{\Delta B}{B} e^{-\frac{(t-t_c)^2}{T^2}}, \quad (28)$$

where  $\Delta B \leq B$  is the catastrophe magnitude as manifested in the change of the reproduction rate,  $t_c$  is the time when the catastrophe reaches its maximum, and  $T$  is the catastrophe duration. Figure 3 shows the numerically found instantons for several values of the catastrophe duration  $T$ . We compared the numerically found action (27) to (the logarithm of) the increase of the extinction

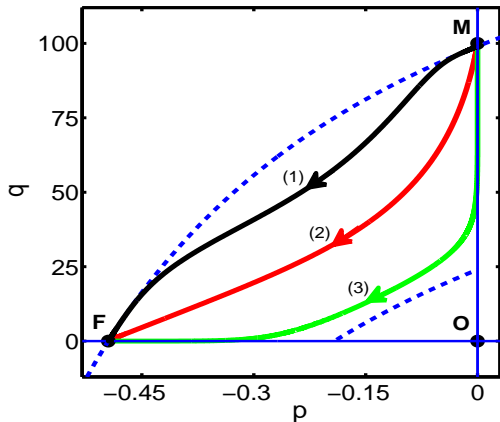


FIG. 3: (Color online.) “Extinction instantons” found by solving the Hamilton equations (23) and (24) numerically for  $f(t)$  given by Eq. (28). The parameters are  $N = 200$ ,  $B = 2$ ,  $\Delta B = 0.75$ , and  $t_c - t_{in} = 40$ . The catastrophe durations are  $T = 1$  (solid line 1),  $T = 3$  (solid line 2) and  $T = 20$  (solid line 3). The upper dashed line is the instanton when there is no catastrophe and  $f(t) = 1 = \text{const}$ . The lower dashed line is the instanton for the system with  $B$  replaced by  $B - \Delta B = \text{const}$ . The upper and lower dashed lines yield the upper and lower bounds, respectively, on the action as a function of  $T$ .

probability due to the catastrophe,  $\Delta\mathcal{P}_0$ , determined by solving numerically the master equation (21) with  $f(t)$  from Eq. (28). Such a comparison is presented in Sec. 4.

### B. Instanton calculations: analytically soluble example

We present now an example when the eikonal equations, describing the impact of a catastrophe on the population extinction probability, are exactly soluble. We assume that the reproduction rate  $\lambda_n$  drops instantaneously to zero at  $t = 0$  and recovers to the pre-catastrophe value, again instantaneously, after time  $T$  has elapsed. In terms of the function  $f(t)$  we have

$$f(t) = \begin{cases} 1 & \text{if } t < 0 \text{ or } t > T, \\ 0 & \text{if } 0 < t < T, \end{cases} \quad (29)$$

see Fig. 4. With this  $f(t)$  the solution of the deterministic rate equation (25) is

$$n(t) = n_s \times \begin{cases} [B(e^t - 1) + 1]^{-1}, & 0 < t < T, \\ [B(e^T - 1)e^{-(B-1)(t-T)} + 1]^{-1}, & t > T, \end{cases} \quad (30)$$

where  $n(t = 0) = n_s = N(1 - 1/B)$  corresponds to the mean-field point  $M$ . The deterministic solution, shown in Fig. 5, predicts a complete recovery of the population after the catastrophe. However, the stochastic effects, missed by the rate equation, can be greatly enhanced

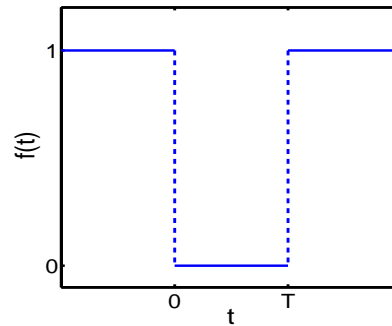


FIG. 4: (Color online.) A model catastrophic event for which the eikonal problem is exactly soluble. The catastrophe starts at time  $t = 0$ , when the reproduction rate drops to zero, and ends at  $t = T$ , when the reproduction rate recovers to its pre-catastrophe value.

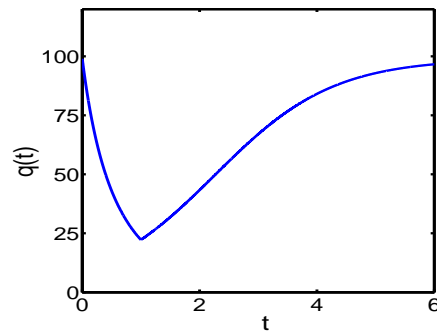


FIG. 5: (Color online.) Effect of the catastrophic event, described by Eq. (29), on the expected population size as predicted by the solution (30) of the deterministic rate equation (25). The parameters are  $N = 200$ ,  $B = 2$ , and  $T = 1$ .

because of the temporary decline in the population size. As a result, they can increase the extinction probability considerably. As we rely on the eikonal approximation in describing this effect, we are interested in the regime where, in spite of the catastrophe, the expected population size by the end of the catastrophe,  $n(T)$ , is still sufficiently large:  $n(T) \gg 1$ .

Because of the special shape of the function  $f(t)$ , there are now two distinct Hamiltonians: the unperturbed Hamiltonian (10) before and after the catastrophe and the zero-reproduction-rate Hamiltonian during the catastrophe:

$$H_c(p, q) = -p \left[ \frac{B}{N}(p+1)q + 1 \right] q. \quad (31)$$

Each of the two Hamiltonians is an integral of motion on the corresponding time interval. The instanton can be found by matching three separate trajectory segments: the pre-catastrophe, catastrophe and post-catastrophe segments. Figure 6 shows a projection of the instanton on the  $(p, q)$  plane. To recall, the instanton must exit, at

$t = -\infty$ , the mean-field point  $M$  and enter, at  $t = \infty$ , the fluctuational point  $F$ . The matching conditions at times  $t = 0$  and  $t = T$  are provided by the continuity of the functions  $q(t)$  and  $p(t)$ . The pre- and post-catastrophe segments must have a zero energy,  $E = 0$ , so they are parts of the original zero-energy trajectory of the unperturbed problem, see Eq. (14). For the catastrophe segment, however, the energy  $E = E_c$  is non-zero and *a priori* unknown. It parametrizes the intersection points  $p_1$  and  $p_2$  (see Fig. 6) between the unperturbed zero-energy line

$$q_0(p) = N - \frac{N}{B(1+p)}, \quad (32)$$

and the non-zero-energy line  $H_c = E_c$ :

$$q_c(p, E_c) = \frac{N}{2B(1+p)} \left[ \sqrt{1 - \frac{4E_c(1+p)B}{Np}} - 1 \right]. \quad (33)$$

Solving the algebraic equation  $q_0(p) = q_c(p, E_c)$  for  $p$ , we obtain

$$p_1(E_c) = -\frac{B-1}{2B} \left[ 1 - \sqrt{1 - \frac{4E_c B}{N(B-1)^2}} \right],$$

$$p_2(E_c) = -\frac{B-1}{2B} \left[ 1 + \sqrt{1 - \frac{4E_c B}{N(B-1)^2}} \right]. \quad (34)$$

To determine  $E_c$  we demand the duration of the catastrophe to be  $T$ . Using Eq. (24) for  $f(t) = 0$  and Eq. (33), we obtain an algebraic equation for  $E_c = E_c(T)$ :

$$\int_{p_1(E_c)}^{p_2(E_c)} \frac{dp}{p [(2B/N)(p+1)q_c(p, E_c) + 1]} = T, \quad (35)$$

where  $q_c(p, E_c)$  is given by Eq. (33). The net increase of the extinction probability of the population due to the catastrophe is proportional to  $\exp[-\mathcal{S}(T)]$ , where the action  $\mathcal{S}(T)$  is

$$\mathcal{S}(T) = \int_{1/B-1}^{p_2[E_c(T)]} q_0(p) dp + \int_{p_2[E_c(T)]}^{p_1[E_c(T)]} q_c[p, E_c(T)] dp + \int_{p_1[E_c(T)]}^0 q_0(p) dp - E_c(T) T. \quad (36)$$

We can also rewrite this action as

$$\mathcal{S}(T) = \mathcal{S}_0 - \int_{p_2[E_c(T)]}^{p_1[E_c(T)]} \{q_0(p) - q_c[p, E_c(T)]\} dp - E_c(T) T, \quad (37)$$

where  $\mathcal{S}_0$  is the unperturbed action, see Eqs. (15) and (16), and the integral term in this equation corresponds to the area of the shaded region in Fig. 6.

To obtain more visual results, let us consider the limit of  $B-1 \ll 1$ . In this limit the pre- and post-catastrophe

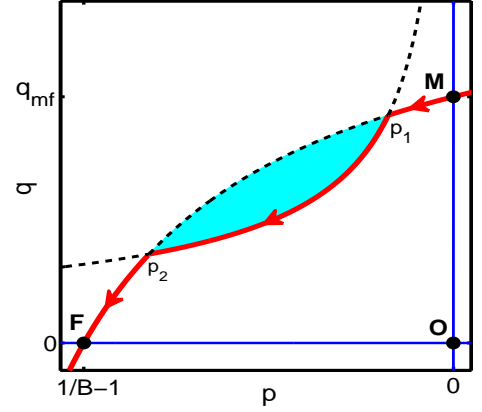


FIG. 6: (Color online.) Projection on the  $(p, q)$  plane of the “extinction instanton” (the thick solid line going from  $M$  to  $F$ ) for the catastrophic event described by Eq. (29). Points  $p_1$  and  $p_2$  correspond to times  $t = 0$  and  $t = T$  where the catastrophic event begins and ends, respectively. At  $t < 0$  and  $t > T$  the instanton follows the zero-energy heteroclinic trajectory  $q = q_0(p)$ , whereas at  $0 < t < T$  it follows a non-zero-energy trajectory  $q = q_c(p, E_c)$ . The energy  $E_c = E_c(T)$  is determined by the given catastrophe duration  $T$ . The area of the shaded region corresponds to the integral term in Eq. (37).

Hamiltonian reduces to the universal Hamiltonian (18). Furthermore, as the terms  $(B/N)pq$  and  $(B/N)q$  can be neglected here compared to 1 in Eq. (31), the zero-reproduction-rate Hamiltonian during the catastrophe simplifies drastically:

$$H_c(p, q) \simeq -pq, \quad (38)$$

and the catastrophe segment of the instanton trajectory becomes simply

$$q_c(p, E_c) \simeq -\frac{E_c}{p}. \quad (39)$$

The corresponding Hamilton equation for  $p$  [Eq. 24], on the catastrophe segment, is  $\dot{p} \simeq p$ , so  $\ln(p_2/p_1) \simeq T$  and

$$\frac{p_2}{p_1} \simeq \exp(T). \quad (40)$$

In their turn,  $p_1 = p_1(E_c)$  and  $p_2 = p_2(E_c)$  are the roots of the equation  $q_0(p) = q_c(p, E_c)$  which now reads

$$N(B-1+p) \simeq -\frac{E_c}{p}. \quad (41)$$

Equations (40) and (41) yield

$$p_1 \simeq \frac{1-B}{e^T + 1}, \quad p_2 \simeq \frac{(1-B)e^T}{e^T + 1}, \quad (42)$$

and

$$E_c \simeq \frac{N(B-1)^2}{4} \cosh^{-2} \left( \frac{T}{2} \right). \quad (43)$$

One can see that, as  $T \rightarrow 0$ , the intersection points  $p_1$  and  $p_2$  merge signaling no change of the unperturbed action. As  $T \rightarrow \infty$ ,  $p_1$  approaches the mean-field point  $M$ , whereas  $p_2$  approaches the fluctuational point  $F$ . In the latter case the population quickly dies out.

Now we use Eq. (37) to calculate the extinction action caused by the catastrophe. After a simple algebra we obtain

$$\mathcal{S}(T) \simeq \frac{2\mathcal{S}_0}{1 + e^T}, \quad (44)$$

where the unperturbed action  $\mathcal{S}_0$  is given by Eq. (17). For short catastrophe durations,  $T \ll 1$ , we obtain a small correction, linear in  $T$ , to the unperturbed action:

$$\mathcal{S}(T) \simeq \mathcal{S}_0(1 - T/2). \quad (45)$$

For long catastrophes,  $T \gg 1$ , the total action  $\mathcal{S}(T)$  decays exponentially with an increase of  $T$ ,

$$\mathcal{S}(T) \simeq 2\mathcal{S}_0 e^{-T}, \quad (46)$$

signaling a rapid extinction.

Interestingly, one can express the extinction action (44) in terms of an *effective* universal Hamiltonian that is catastrophe-free. Indeed, Eq. (44) can be interpreted as the area of a right-angled triangle:

$$\mathcal{S}(T) \simeq \frac{B-1}{2} n_{eff}(T), \quad (47)$$

where  $(B-1)$ , the absolute value of  $p$  at the fluctuation point  $F$  (for  $B-1 \ll 1$ ), is one of the legs of the triangle. The other leg,  $n_{eff}(T)$ , is the harmonic mean of  $n_s$  and  $n(T)$ :

$$\frac{2}{n_{eff}(T)} = \frac{1}{n_s} + \frac{1}{n(T)}. \quad (48)$$

[To recall, close to the bifurcation  $n_s \simeq N(B-1)$  is the steady-state pre- and post-catastrophe population size and  $n(T) \simeq n_s \exp(-T) < n_s$  is the population size immediately after the catastrophe, as predicted by the deterministic rate equation.] For short catastrophes  $n(T)$  is close to  $n_s$ , and one obtains a small correction to the unperturbed action. For long catastrophes  $n(T) \ll n_s$ , and  $n_{eff}(T) \simeq 2n(T)$ . We are unaware of a simpler way to arrive at these results via arguments based on the deterministic description of the catastrophe, Eq. (30), and on the knowledge of the unperturbed action, Eq. (17).

For the eikonal approximation to be valid, we have to demand that both the total action, and the correction to it caused by the catastrophe, be much larger than unity. This yields a range of rescaled catastrophe durations

$$\mathcal{S}_0^{-1} \ll T \ll \ln \mathcal{S}_0 \quad (49)$$

which becomes broader as  $\mathcal{S}_0 \gg 1$  increases.

The eikonal theory provides, with exponential accuracy [26], the value of the increase of the extinction probability  $\Delta \mathcal{P}_0 \equiv \mathcal{P}_0^* - \mathcal{P}_0^B$  (see Section I) in terms of the ‘‘catastrophe action’’  $\mathcal{S}(T)$ :

$$\Delta \mathcal{P}_0 \propto e^{-\mathcal{S}(T)}. \quad (50)$$

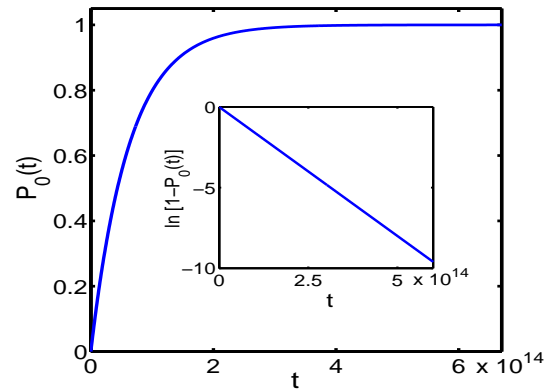


FIG. 7: (Color online.) The extinction probability  $\mathcal{P}_0(t)$  vs. time if there is no catastrophe. The parameters are  $N = 10,800$  and  $B = 1.08$ . Inset:  $\ln[1 - \mathcal{P}_0(t)]$  vs. time. The slope of this graph yields the MTE:  $\tau \simeq 6.2 \times 10^{13}$ , so that  $\ln \tau \simeq 31.8$ . For comparison, the eikonal theory, see Eq. (16), predicts  $\ln \tau \simeq 30.4$ .

#### IV. COMPARISON TO NUMERICAL SOLUTIONS OF THE MASTER EQUATION

We tested the predictions of the eikonal theory by solving the (truncated) master equation (3) numerically. We observed that, if there is no catastrophe, the system approaches a quasi-stationary probability distribution after a time  $\mathcal{O}(\tau_0)$ , as expected. This probability distribution then very slowly decays in time, while the extinction probability  $\mathcal{P}_0(t)$  very slowly grows. The corresponding decay/growth time is in good agreement with the MTE  $\tau$  predicted from Eq. (16), see Fig. 7.

We modeled the catastrophe by multiplying the unperturbed reproduction rate by  $f(t)$ , with  $f(t)$  from either Eq. (28), or Eq. (29). The validity of the eikonal approximation demands  $\mathcal{S}_0 \gg 1$ . [One must also demand that the expected population size in the quasi-stationary state be much larger than unity:  $q_{mf} = N(B-1)/B \gg 1$ . However, above the bifurcation point  $B > 1$ , when the deterministic version of the Verhulst model has a non-trivial attracting fixed point, the criterion  $\mathcal{S}_0 \gg 1$  is always more restrictive.] One more criterion for the validity of the eikonal approximation is  $\mathcal{S}(T) \gg 1$ , for all values of  $T$  that we used.

In our numerical solutions of the master equation the initial condition corresponded to a fixed population size:  $\mathcal{P}_n(t=0) = \delta_{n,n_0}$ , where  $\delta_{n,n_0}$  is the Kronecker delta, and  $n_0 \gg 1$ . In this case an immediate extinction before relaxing to the quasi-stationary state has an exponentially small probability. The catastrophe time  $t_c$  was chosen to be several times longer than the relaxation time  $\tau_0$  for the chosen parameters, but *much* shorter than the expected MTE. Finally, the catastrophe duration  $T$  was chosen such that the correction to the action caused by the catastrophe and the total action satisfy the conditions  $\mathcal{S}_0 - \mathcal{S}(T) \gg 1$  and  $\mathcal{S}(T) \gg 1$ . In the exactly soluble case,



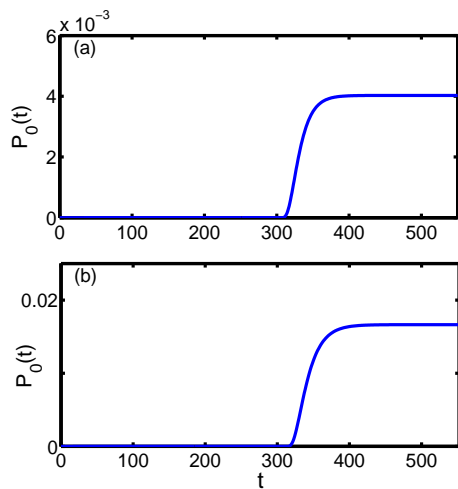


FIG. 8: (Color online.) The extinction probability  $\mathcal{P}_0(t)$  vs. time (at times much smaller than the MTE  $\tau$ ), found by solving numerically the (truncated) master equation (21) with  $f(t)$  from Eq. (29). (a):  $N = 14, 400$ ,  $B = 1.08$  and  $T = 2.5$ . (b):  $N = 10, 800$ , the rest of parameters is the same as in (a). The starting time of the catastrophe in both cases,  $t_c = 300$ , obeys the condition  $t_r \ll t_c \ll \tau$ .  $\mathcal{P}_0(t)$  before the catastrophe is negligibly small and cannot be seen in this scale.

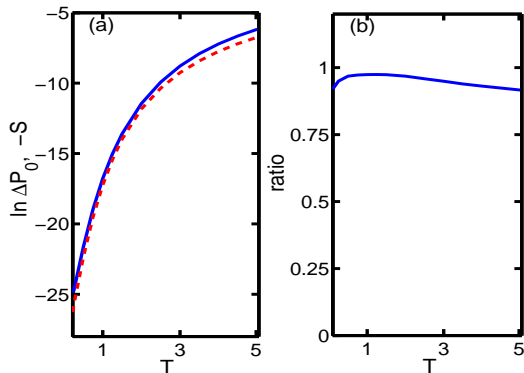


FIG. 9: (Color online.) (a) A comparison between the natural logarithm of the net contribution  $\Delta\mathcal{P}_0$  of the catastrophe to the extinction probability  $\mathcal{P}_0(t)$  (see text), and  $-\mathcal{S}(T)$  from Eq. (27) vs.  $T$ . (b) The ratio of the two quantities vs.  $T$ . The parameters are  $N = 200$  and  $B = 2$ ,  $\Delta B = 0.75$ , and  $t_c - t_{in} = 40$ .

presented at the end of the previous section, these two inequalities reduce to the double inequality (49). Figure 8 presents, for two different sets of parameters, our numerical results for  $\mathcal{P}_0(t)$ . Here  $f(t)$  is given by Eq. (29).

Figures 9 and 10 compare the predictions of our eikonal theory with the numerical solutions of the master equation. To estimate the direct impact of the catastrophe on the extinction probability we calculated the quantity

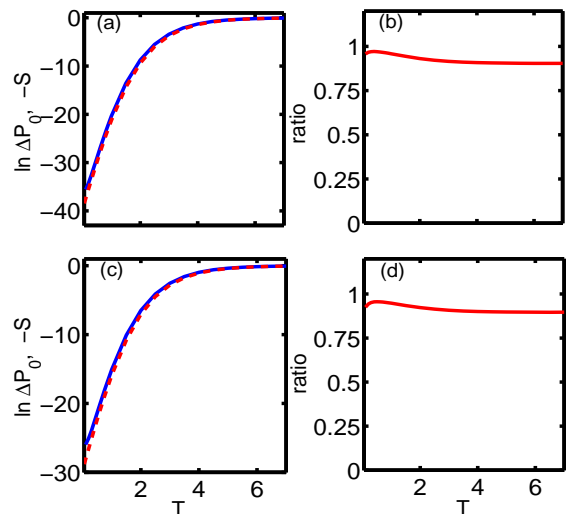


FIG. 10: (Color online.) The natural logarithm of the numerically computed  $\Delta\mathcal{P}_0$  vs.  $T$  (solid line) is compared to  $-\mathcal{S}(T)$  predicted by Eq. (44) (dashed line). The parameters in (a) and (c) are the same as in Fig. 8 (a) and (b), respectively. In (b) and (d) the ratios of the same quantities,  $\ln \Delta\mathcal{P}_0$  and  $-\mathcal{S}(T)$ , are plotted vs.  $T$  for the same parameters as in (a) and (c), respectively. The analytical result in (b) deviates from the numerical result by 2.8% at the maximum. The corresponding deviation in (d) is 4.4% indicating that, as  $\mathcal{S}_0$  increases, the agreement between the analytical and numerical results improves.

$\Delta\mathcal{P}_0 \equiv \mathcal{P}_0^* - \mathcal{P}_0^B$ , where  $\mathcal{P}_0^B$  is the measured extinction probability before the catastrophe starts but after the relaxation stage ends. As  $t_c \ll \tau$ , most of the contribution to  $\mathcal{P}_0^B$  comes, for the parameters and initial conditions we worked with, from the projections of the initial condition on the (rapidly decaying) higher eigenmodes of the system, see [5, 6].

Our numerical results for  $f(t)$  from Eq. (28) are presented in Fig. 9. The figure compares  $\ln \Delta\mathcal{P}_0(T)$  and  $-\mathcal{S}(T)$  found by solving the eikonal equations numerically, see Section 3.1. Figure 10 corresponds to the simple catastrophe described by Eq. (29). Here  $\ln \Delta\mathcal{P}_0(T)$  is compared to  $-\mathcal{S}(T)$  for the two sets of parameters used in Fig. 8. These two sets of parameters were chosen to obey the strong inequality  $B - 1 \ll 1$ , so that we could test the analytical prediction (44). Good agreement between the theory and numerical computations is observed in all cases, over a broad range of  $T$ . One can see from Fig. 9 (b) and Figs. 10 (b) and (d) that the agreement is best for intermediate values of  $T$  and deteriorates for small and large values of  $T$ . This behavior is consistent with the validity criteria of the eikonal approximation: for too a small  $T$  the inequality  $\mathcal{S}_0 - \mathcal{S}(T) \gg 1$  does not hold, whereas for too a large  $T$  the inequality  $\mathcal{S}(T) \gg 1$  does not hold. The quantity  $-(\ln \Delta\mathcal{P}_0)/\mathcal{S}$  includes information about the pre-exponent  $A(T)$  of the complete relation  $\Delta\mathcal{P}_0 = A(T)e^{-\mathcal{S}(T)}$ . This pre-exponent has not yet been determined theoretically.

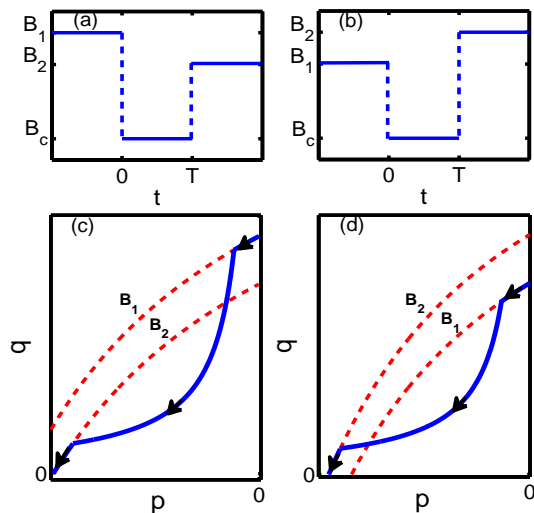


FIG. 11: (Color online.) Not fully reversible catastrophes, as reflected in the reproduction rate vs. time, and the extinction instantons for  $B_1 > B_2$  (a and c) and  $B_1 < B_2$  (b and d). The solid lines in (c) and (d) are the instantons, the dashed lines are the zero-energy lines, see Eq. (14), for  $B = B_1$  and  $B = B_2$ .

## V. SUMMARY AND DISCUSSION

This work shows that eikonal approximation to the evolution equation for the probability generating function provides a robust and efficient way of evaluating the impact of catastrophic changes, reflected in the reproduction rates, on the stochastic population dynamics.

The theory presented in this paper is non-perturbative

in the catastrophe magnitude. For relatively weak and/or short catastrophes one can develop an eikonal *perturbation* theory by assuming that the correction to the unperturbed action  $\mathcal{S}_0$  is small compared to the unperturbed action itself (but still much larger than unity, so that the eikonal theory is valid). For a time-periodic modulation of the reaction rates such a theory has been recently developed in Refs. [27, 28]. We checked that, for the exactly soluble catastrophe model, presented at the end of section III, such a perturbation theory correctly predicts the small- $T$  asymptote of the action, Eq. (45).

Although the examples that we have considered dealt with fully reversible catastrophes, the eikonal method is extendable to more complicated situations. As an example, consider the case when the reproduction rate  $B$  reaches, after a catastrophe ends, a value  $B_2$  different from the pre-catastrophe value  $B_1$ . The extinction instantons, and the corresponding total actions, can be easily found for  $B_1 > B_2$  and for  $B_1 < B_2$ , see Fig. 11. This immediately yields, with exponential accuracy, the corresponding increase in the extinction probability caused by the catastrophe.

## Acknowledgments

We thank Boris Shklovskii for a useful discussion. M. A. is supported by the Clore Foundation; M. A. and B. M. were supported by the Israel Science Foundation (Grant No. 408/08); A. K. was supported by the NSF grant DMR-0405212 and by the A. P. Sloan foundation. M. A. and B. M. are grateful to FTPI of the University of Minnesota for hospitality.

- 
- [1] S. R. Beissinger and D. R. McCullough (Editors), *Population Viability Analysis* (University of Chicago Press, Chicago, 2002).
  - [2] C.W. Gardiner, *Handbook of Stochastic Methods* (Springer Verlag, Berlin, 2004).
  - [3] N.G. van Kampen, *Stochastic Processes in Physics and Chemistry* (North-Holland, Amsterdam, 2001).
  - [4] V. Elgart and A. Kamenev, Phys. Rev. E **70**, 041106 (2004).
  - [5] M. Assaf and B. Meerson, Phys. Rev. Lett. **97**, 200602 (2006).
  - [6] M. Assaf and B. Meerson, Phys. Rev. E **75**, 031122 (2007).
  - [7] L.D. Landau and E.M. Lifshitz, *Quantum Mechanics: Non-Relativistic Theory* (London, Pergamon, 1977), Chapter 3.
  - [8] B. Gaveau, M. Moreau, and J. Tòth, Lett. Math. Phys. **37**, 285 (1996).
  - [9] C.R. Doering, K.V. Sargsyan and L.M. Sander, Multi-scale Model. and Simul. **3**, 283 (2005).
  - [10] G.H. Weiss and M. Dishon, Math. Biosci. **11**, 261 (1971).
  - [11] A. D. Barbour, Adv. Appl. Probab. **8**, 296 (1976).
  - [12] I. Oppenheim, K. E. Shuler, G. H. Weiss, Physica **88A**, 191 (1977).
  - [13] R.J. Kryscio and C. Lefèvre, J. Appl. Probab. **26**, 685 (1989).
  - [14] I. Näsell, J. Theor. Biol. **211**, 11 (2001).
  - [15] V. Elgart and A. Kamenev, Phys. Rev. E **74**, 041101 (2006).
  - [16] M. Assaf and B. Meerson, Phys. Rev. E **74**, 041115 (2006).
  - [17] A. Kamenev and B. Meerson; arXiv:0801.4900v1 (2008).
  - [18] M. I. Freidlin and A. D. Wentzell, *Random Perturbations of Dynamical Systems* (Springer-Verlag, New York, 1984).
  - [19] R. Graham, edited by F. Moss and P. V. E. McClintock, *Noise in Nonlinear Dynamical Systems* (Cambridge University Press, Cambridge, 1989).
  - [20] M.I. Dykman, E. Mori, J. Ross, and P.M. Hunt, J. Chem. Phys. **100**, 5735 (1994).
  - [21] The spectral method [5, 6, 16] also yields the pre-exponent that is lacking in Eq. (16). The pre-exponent coincides with that found, in the same limit, in Refs. [9, 14].

- [22] M. Dykman, I. B. Schwartz, and A. S. Landsman, Phys. Rev. Lett. **101**, 078101 (2008).
- [23] I. Näsell, Mathematical Biosciences **179**, 1 (2002).
- [24] O. A. van Herwaarden, J. Math. Biol. **35**, 793 (1997).
- [25] I. Näsell, J. Royal Stat. Soc. B **61**, 309 (1999).
- [26] More precisely, the theory yields an exact value of the limit of  $\ln(\Delta\mathcal{P}_0)/N$  as  $N \rightarrow \infty$ .
- [27] C. Escudero and J.Á. Rodríguez, Phys. Rev. E **77**, 011130 (2008).
- [28] M. Assaf, A. Kamenev and B. Meerson; arXiv:0807.4812L.